Solubility of Indium-Tin Oxide in simulated lung and gastric fluids: Pathways for human intake

Jens Christian Østergård Andersen*, Alastair Cropp[1], and Diane Caroline Paradise[2]

Camborne School of Mines, University of Exeter, Penryn Campus, Penryn, TR10 9FE, Cornwall, United Kingdom. Email J.C.Andersen@exeter.ac.uk

* Corresponding author

1. Currently at: Carl Zeiss Ltd, 509 Coldhams Lane, Cambridge, CB1 3JS, United Kingdom email al.cropp@zeiss.com

2. Current address: 15 Wendron Street, Helston, Cornwall, TR13 8PT, United Kingdom email paradise3691@hotmail.com

Key words: Indium, indium-tin oxide, lung, gastric, environmental dispersion, electronic waste

Acknowledgments

This paper was in part supported by the Natural Environment Research Council (NERC, NE/L001896/1). The authors benefited from advice from and discussions with Dr Adam Feldman, sample preparation and X-ray diffraction by Dr Gavyn Rollinson, and ICP-MS analysis by Sharon Uren.

Abstract

From being a metal with very limited natural distribution, indium (In) has recently become disseminated throughout the human society. Little is know of how In compounds behave in the natural environment, but recent medical studies link exposure to In compounds to elevated risk of respiratory disorders. Animal tests suggest that exposure may lead to more widespread damage in the body, notably the liver, kidneys and spleen. In this paper, we investigate the solubility of the most widely used In compound, indium-tin oxide (ITO) in simulated lung and gastric fluids in order to better understand the potential pathways for metals to be introduced into the bloodstream. Our results show significant potential for release of In and tin (Sn) in the deep parts of the lungs (artificial lysosomal fluid) and digestive tract, while the solubility in the upper parts of the lungs (the respiratory tract or tracheobronchial tree) is very low.

Our study confirms that ITO is likely to remain as solid particles in the upper parts of the lungs, but that particles are likely to slowly dissolve in the deep lungs. Considering the prolonged residence time of inhaled particles in the deep lung, this environment is likely to provide the major route for uptake of In and Sn from inhaled ITO nano- and microparticles. Although dissolution through digestion may also lead to some uptake, the much shorter residence time is likely to lead to much lower risk of uptake.

1. Introduction

There is increasing evidence to suggest that indium (In) compounds may be harmful to human health, yet the potential transfer mechanisms into the human body are very poorly understood. While in vivo tests on mice and rats have shown that In-phosphide, In-arsenide In-trichloride and In-acetate have toxic and carcinogenic effects (Chapin et al., 1995; Oda, 1997; Tanaka, 2004, Lee et al., 2016), the most widely used compound, indium-tin oxide (ITO), was until recently considered to be comparably inert (Fowler et al., 2009). However, studies by Homma et al. (2003) and Cummings et al. (2010, 2016) linked health problems and fatalities among factory workers to their exposure to ITO. Indeed, mounting evidence from recent research suggests that exposure to ITO can be directly linked to lung disorders, such as pulmonary alveolar proteinosis, pulmonary fibrosis, emphysema, and pneumothoraces (Chonan et al., 2007; Lison et al., 2009; Nakano et al., 2009; Omae et al., 2011, Cummings et al., 2012, 2016; Badding et al., 2015, 2016). Experiments on rats by Nagano et al. (2011) furthermore indicate that exposure to ITO may linked to increased risk of malignant lung tumors.

Despite the very low solubility of ITO, Chonan et al. (2007) and Hamaguchi et al. (2008) found elevated concentrations of In in serum from current and former workers exposed to ITO at a factory in Japan. These studies suggest that the ITO does not remain entirely inert upon intake, but that In is released to circulate more widely within the human body. Very little research has been carried out to document any wider health effects, but Omura et al. (2002) suggested that exposure to ITO may lead to testicular toxicity in hamsters. Bomhard (2016), however, suggested that damage to the male sexual organs may be a secondary effect from the lung damage. In more general terms, Smith et al. (1978) and Blazka (1998) suggest that chronic exposure to In may lead to weight loss and damage to the

liver, kidneys and spleen, and it is likely that once In from ITO enters the bloodstream, it may have similar effects as ionic or colloidal In compounds (cf., Smith et al., 1978, Blazka, 1998).

In this study, we report the results of in vitro experiments to examine the dissolution behavior of ITO in simulated lung and gastric fluids and discuss the potential transfer mechanisms for In and associated tin (Sn) into the human body.

2. Background

Indium is a metal that belongs to group 13 of the periodic table along with boron, aluminum, gallium and thallium. The principal oxidation state is trivalent and the effective ionic radius for In^{3+} in 8-fold coordination is 0.092 nm (Shannon, 1976), which is intermediate between scandium and the lanthanides. The metal is predominantly found in sulfide minerals that are unstable under oxidizing conditions at the Earth's surface. Consequently it is likely to be released during acid mine drainage. Tin in contrast occurs principally in the form of cassiterite (SnO_2) which is very stable in the environment and tends to be residual after weathering.

Indium is very rare in the natural environment and has historically had very little use in society. Tin in contrast, although also naturally rare, has a history of human exploitation that dates back millennia, and it's environmental and health effects are much better constrained. However, through the distribution of mobile electronic devices, flat-screen televisions and computer displays, In has over the last decade appeared extensively in the human environment (White and Hemond, 2012). As a consequence, the global potential for exposure has increased dramatically, and concerns about environmental and health issues must be considered with some urgency.

The most widespread use of In is in sintered indium-tin oxide (ITO), which is applied as a conductive coating on flat-screen liquid crystal displays in mobile electronic devices,

computer monitors and televisions. Indium is also used in lead-free solders, light-emitting diodes, and copper-indium-gallium-selenide (CIGS) photovoltaic panels. As flat screen displays are now almost completely replacing cathode-ray televisions and computer monitors, and mobile electronic devices are becoming more widespread, ITO can be expected to start appearing in the domestic waste stream in significant quantities. Flat screen displays contain on average 234 mg In per square meter (Böni and Widmer, 2011); the average lifetime of a mobile electronic device is estimated to less than 5 years, while the lifetime of a domestic flat panel television or computer monitor is estimated to 9 years (USEPA, 2011). While a significant proportion of computer monitors are recycled (38%), televisions and mobile telephones have very poor recycling statistics (17% and 8% respectively, USEPA, 2011) and mostly end up in the household waste. The global end-of-life recycling rate for In was estimated to be less than 1% in 2011 (Graedel et al., 2011).

During the lifetime of a flat-screen display, the ITO is not exposed, and it therefore does not pose immediate risk to general consumers. Apart from during manufacture, the main risks for release of ITO particles would be during recycling and disposal of the devices, where ITO coated glass is typically mechanically abraded before In is recovered by chemical leaching (Zeng et al, 2015; Zhang et al., 2015).

The biological residence time of ITO particles in the body is a significant parameter to consider in relation to intake. Only a small fraction of insoluble particles are likely to be retained within the upper respiratory tract or tracheobronchial tree (Patrick and Stirling, 1977; Watson and Brain, 1979; Gore and Patrick, 1982). However, as particles are introduced to the deep lung environment (the bronchioles and alveoli), they are likely to accumulate over extensive periods of time. Radford and Martell (1977) estimated that the residence time for insoluble particles in bronchial tissue derived from cigarette smoke amounted to 3 to 5 months. The digestive system, in contrast, has a much shorter transit time, with solid particles

being excreted typically after one to three days (Daugherty and Mrsny, 1999). Morrow et al. (1957) determined the biological half-life of In_2O_3 in rats (administrated orally or by inhalation) to be in the order of 9-10 days, however, a recent study by Amata et al. (2015) suggests that the actual residence times of In in humans may be in the order of 8 years.

The United States recommended exposure limits in air are 0.1 mg/m^3 In and 2 mg/m^3 inorganic Sn (NIOSH, 1981), which with an inhalation rate of 20-25 m^3/day for an average weight adult male (Brochu et al., 2006) would equate to a maximum accumulation in the lungs of 0.67-0.83 mg In for an eight hour working day (probably as high as 1 mg In for obese adults). With less than 10 wt% SnO_2, the inhalation of Sn from ITO is much less of an issue. The regulated exposure limit for In in Japan is much more restrictive at 0.0003 mg/m^3 (MHLW, 2010). The United States minimal risk level for oral intake of inorganic Sn is 0.3 mg/kg/day (ATSDR, 2016) while no safe level appears to have been identified for In.

3. Materials and Methods

For this study, we used ITO powder (<44 μm, 325 mesh, ≥ 99.99% purity trace metal basis, Sigma Aldrich 494682-25G, CAS 50926-11-9:d 1.2) listed to have a composition of 90 wt% In_2O_3 and 10 wt% SnO_2. The powder is similar in composition and particle size to the material used to produce ITO sputtering targets (Falk, 2012). The production of sputtering targets involves the densification of the ITO particles under pressure and at high temperature to form a granular solid with or without binders or additives (Falk, 2012). During sputtering, nanoparticles are released through heating of the target to deposit as a thin conductive coating on the substrate (Tuna et al., 2010). The coating consists of nanoparticles that are typically tens of nanometers across (Kim et al., 2000).

The powder was investigated by powder X-ray diffraction (XRD) and electron-probe microanalysis (EPMA) at Camborne School of Mines, University of Exeter, to establish the

151 structure and variability and particularly to confirm that the material had been sintered. The
152 XRD was conducted on a Siemens D5000 equipped with the Bruker Topas software using the
153 JCPDS database (ICDD, 2004). The EPMA analysis was carried out on the JEOL JXA-8200
154 using a 30 nA electron beam accelerated to 15 kV and wavelength-dispersive X-ray
155 spectrometers. Results were quantified with tin metal, indium-arsenide, and wollastonite
156 standards using the CITZAF routine (Armstrong, 1995).

157 Dissolution experiments were carried out in screw-capped polypropylene beakers
158 (SCP Science DigiTUBES, product 010-500-261). Samples were prepared in triplicate with a
159 procedural blank for each set. Experiments were designed to simulate key environments that
160 are considered to be significant routes for particle intake. A set of control experiments were
161 carried out with ITO in deionised water (purified with an Elga/Veolia Purelab Flex system).

162 The gastric environment was simulated with the physiologically based extraction test
163 (PBET) solution of Ruby et al. (1996), however our experiments were conducted without
164 suspended particles or gas flow. Tests were conducted for up to four hours, exceeding the
165 maximum residence time of food in a child's stomach (Ruby et al., 1996). The pH of the
166 solution was adjusted to 4 using concentrated HCl, as this value was considered intermediate
167 between the conditions of fasting and full. A separate test was carried out with trypsin in
168 deionised water at neutral pH, as a simplistic way of testing if digestive enzymes may
169 facilitate further dissolution.

170 The lung environment was explored using the formulations of Colombo et al. (2008):
171 Gamble's solution is used to simulate the conditions as ITO particles are inhaled (in the upper
172 respiratory tract and tracheobronchial tree), while artificial lysosomal fluid (ALF) is
173 considered to replicate the more acidic conditions in the deep lung (bronchioles and alveoli).

174 Stock solutions (Table 1) were prepared as specified by Ruby et al. (1996) and
175 Colombo et al. (2008). Particular care was taken to add the components of Gamble's solution

176 in the correct order to avoid salt precipitation. All plastic ware was soaked in dilute HNO_3,
177 rinsed in deionised water and oven dried prior to use in the experiments.
178 Experiments were carried out in triplicate using separate beakers (rather than aliquots
179 from a single beaker) with a procedural blank for each set of three samples. For each
180 experiment, 50 mg of ITO powder was weighed into the polypropylene beakers and 10 ml of
181 the required stock solution added (time zero) using an Eppendorf Research Plus® pipette
182 with non sterile, single use pipette tips. After addition of the fluids, the experiments were
183 sealed, gently swirled to ensure maximum wetting of the ITO powder without leaving ITO
184 particles on the beaker walls, and transferred to an oven at 37ºC. The gastric experiments
185 were carried out with residence times of up to 4 hours, while the lung experiments extended
186 to 480 hours. A separate experiment was conducted to test the influence of enzymes on the
187 digestion, for this experiment, 150 mg ITO and 50 mg trypsin (from porcine pancreas, Sigma,
188 T4799-5G, Lot# 110M7362V) was weighed into the beakers and 25ml of de-ionised water
189 added. The beakers were swirled to ensure complete wetting of the ITO powder and trypsin
190 and placed in an oven at 37ºC. These experiments were carried out with residence times of up
191 to >200 hours.
192 At the termination of each experiment, three sample beakers and one blank were
193 collected and the solution immediately vacuum filtered through a single-use 0.45 µm Teflon
194 membrane (SCP Science DigiFILTER, product 010-500-070) and stored at room temperature
195 prior to analysis. None of the plastic ware was re-used.
196 The samples were analyzed for ^{28}Si, ^{39}K, ^{56}Fe, ^{115}In and ^{118}Sn by the Agilent 7700x
197 quadrupole inductively-coupled mass spectrometer (ICP-MS) at Camborne School of Mines,
198 University of Exeter using ^{45}Sc as internal standard. Samples were introduced in undiluted
199 form using an Agilent ASX-520 autosampler. The ICP-MS was fitted with a Peltier cooled
200 Scott type spray chamber and an inert PTFE sample introduction system. Indium and Sn were

measured with helium as a collision cell gas to suppress polyatomic mass interferences. The CeO^+/Ce^+ was 0.136% and the Ce^{2+}/Ce^+ was 1.372%.

The interference of ^{115}Sn (0.34% of the natural abundance of Sn) on ^{115}In was negligible (< 0.14 ppb) at the measured concentrations. ^{28}Si and ^{56}Fe were used as monitors of potential contamination through handling of reagents and beakers, the Si was systematically below 2µg/g and Fe below 0.5µg/g. The internal standard recovery was 96.6 ± 14.2 %) except for Gamble's solution (117.6 ± 9.0 %). The instrument was calibrated with 1.6, 8, 40, 200, 1000 and 2000 µg/kg solutions, while a 40 µg/kg standard solutions was tested after every 12 analyses to monitor instrument drift. After each analysis, the sample introduction system was flushed with deionized water followed by dilute HNO_3 and a further wash with deionized water. No carryover was observed for the measured metals. Time (*t*) is reported in hours (hrs) and concentrations in parts per billion (ppb, µg/kg) and parts per million (ppm, mg/kg). Element ratios are reported by weight. Errors are reported at the 2σ level.

4. Results

The ITO powder consists of irregularly shaped particles of 10-50 µm that commonly are hollow and have large surface to mass ratios (Figure 1). X-ray diffraction confirmed the powder to be composed of Sn-doped In_2O_3 with distinct signals also for discrete SnO_2. No signals were observed for In_2SnO_5 or $In_4Sn_3O_{12}$ (Kim et al., 2006; Heward and Swenson, 2007). Spot analysis by EPMA confirmed the SnO_2 content of the tin-doped indium oxide to vary between 2.6 and 8.0 wt% (average 3.0 wt%, n=26) and also confirmed the presence of discrete SnO_2 particles that are generally less than 5µm across. The only impurity detected was silicon dioxide (SiO_2) which occurs throughout at 0.4 wt% and locally reaches 2 wt%. The compositions are consisted with material that has been sintered at temperatures in excess

of 1000 °C (Heward and Swenson, 2007), and is as such similar to industrial ITO powder used for the production of sputtering targets. The wall thicknesses of the individual ITO particles are up to to 3μm, which is generally thicker than the average 125 nm for ITO coatings (Böni and Widmer, 2011). So while the powder is compositionally and structurally similar to industrial ITO, the greater wall thicknesses lead to lower expected surface to volume ratios than for particles liberated from ITO coatings. The powder furthermore displays no signs of having been subjected to the densification that is involved in the production of ITO sputtering targets. The particle sizes and shapes therefore differ to those that can be expected to be released from ITO sputtering targets or ITO coatings during production or recycling. We consider that the structural and compositional similarities are reasonable matches to industrial ITO. The particle size differences and lack of densification, however, are likely to lead to minor differences in the dissolution kinetics. Although the dissolution speed may differ, we have no reason to believe that the metal concentrations in the fluids would be substantially different.

The results of the dissolution experiments are presented in Figures 2-7 and the supplementary data file. As per design, all samples had significant excess of undissolved ITO at the termination of the experiments. Since partial dissolution is a fractional process, it is appropriate at least as a first approximation, to consider the dissolution curves as power functions (cf., Lánský and Weiss, 2003). Our results show very limited solubility of ITO in deionized water and under simulated upper respiratory tract conditions (Gamble's solution) but significant solubility in the simulated deep lung (ALF) and digestive (PBET) environments. In deionized water (Figure 2), In concentrations stabilized at 134 ± 47 ppb in less than 18 hours while Sn concentrations systematically remained below 0.2 ppb. Both display decreasing concentrations with time, along the equations In (ppb) = 253 $t^{-0.15}$ and Sn (ppb) = 8.59 $t^{-1.80}$, which can be explained by adsorption to the plastic containers (Robertson,

1968; Smith, 1973). The In blank was measured at 0.18 ± 0.16 ppb while the Sn blank remained below 0.01 ppb.

Under simulated upper respiratory tract conditions (Figure 3), concentrations of In and Sn remained very low. Surprisingly, Sn appeared to be taken into solution more readily than In. Indium remained below 10 ppb and showed a negative correlation with time at In (ppb) = 6.58 $t^{-0.22}$ (R^2 = 0.63), while Sn reached 60 ppb and displaying a positive correlation along Sn (ppb) = 9.69 $t^{0.32}$ (R^2 = 0.87). The In/Sn evolved along a trend of In/Sn (w/w) = 0.68 $t^{-0.54}$ (R^2 = 0.82). As above, the negative correlation of In with time can be explained by adsorption to the container walls (Robertson, 1968; Smith, 1973). The In blank was 3.39 ± 4.06 ppb and the Sn blank was 0.95 ± 0.51 ppb.

The deep lung environment (simulated with the ALF solution), in contrast, displayed significant dissolution of the ITO (Figure 4) with maximum concentrations after 480 hrs reaching 236 ppm In and 8.4 ppm Sn. The increase in concentrations of In and Sn follow best fit regressions of In (ppb) = 4276 $t^{0.61}$ (R^2 = 0.97) and Sn (ppb) = 642 $t^{0.42}$ (R^2 = 0.99). The In/Sn of the fluid increased over time along a best of In/Sn (w/w) = 6.66 $t^{0.18}$ (R^2 = 0.71), showing differential dissolution of In relative to Sn.

The stomach environment (simulated with the PBET solution) similarly displayed significant dissolution of ITO with concentrations increasing systematically over time (Figure 5). Maximum concentrations after 4 hours were 3.6 ppm In and 127 ppb Sn. Regressions are for In (ppb) = 2092 $t^{0.34}$ (R^2 = 0.95) and Sn (ppb) = 72.6 $t^{0.39}$ (R^2 = 0.93). The In/Sn ratio showed little variation over time at In/Sn (w/w) = 28.84 $t^{-0.05}$ (R^2 = 0.36). Blanks were systematically below 1 ppb In and 0.2 ppb Sn.

Experiments with trypsin (Figure 6) showed In reaching a stable concentration of 901 ± 107 ppb in solution in less than 18 hours. The best fit correlation for In (ppb) = 876 $t^{0.01}$ is not convincing (R^2 = 0.01). The Sn concentration displayed a decrease in concentration along

276 a trend of Sn (ppb) = 46.57 $t^{-0.33}$ (R^2 = 0.27). A slight increase in In/Sn (ppb) = 12.5 $t^{0.36}$ (R^2 =
277 0.04) over time is unconvincing. The average of 9 blank measurements yielded 1.67 ± 1.07
278 ppb In and <0.05 ppb Sn.
279 When the different results are compared (Figure 7), it is clear that by far the most
280 extensive potential for release of In and Sn from ITO is in the simulated deep lung
281 environment (Figure 7a, b). Although the dissolution rates were nearly as high in the stomach
282 environment, the much shorter particle residence time effectively limited the concentrations
283 that could be reached. Although In may be subject to further dissolution in the pancreatic
284 juice, the total fluid concentrations that can be reached during digestion remains much lower
285 than the deep lung environment. The simulated upper lung environment displays almost no
286 dissolution of In, while Sn is very weakly soluble – although at a rate that is nearly 100 times
287 lower than in the deep lung environment. Selective leaching, expressed by In/Sn is
288 particularly strong in the upper lung environment (selective leaching of Sn) and in deionised
289 water (selective leaching of In). The simulated deep lung and stomach environments as well
290 as the pancreatic juice are much less selective of metals during leaching.
291
292 **5. Discussion**
293 Although In is more common in the continental crust than silver (Rudnick and Gao,
294 2003), little is known about the environmental dispersal of the most commonly used In
295 compounds (White and Hemond, 2012). Most toxicological studies focus on ITO factories,
296 where workers are exposed to particularly high concentrations of the metal in various forms.
297 While In is primarily recovered through chemical leaching, the recycling business, in
298 particular, employs mechanical abrasion (sand blasting, sanding, wet grinding) to liberate
299 ITO (Hines et al., 2013, Zeng et al., 2015; Zhang et al., 2015), releasing nano- and micro-
300 particles into the air that may be inhaled. Most medical studies consequently focus on

301 respiratory disorders, as recently evaluated by Cummings et al. (2012), who associated ITO
302 with pulmonary alveolar proteinosis, pulmonary fibrosis, emphysema, and pneumothoraces.
303 Although Zheng et al. (1994) suggested that In is poorly absorbed in the body, Nagano et al.
304 (2011) suggested (based on a study of rats) that in addition to the lungs, the metal may also
305 concentrate in the spleen, kidney and liver. The study by Chen (2007) suggests that some In
306 is eventually excreted, and while the study by Morrow et al. (1957) suggests a short
307 biological half-life (in the order of a couple of weeks), Amata et al. (2015) consider that
308 actual residence times in humans to be as high as 8 years. It is worth noting that while the
309 study by Morrow et al. (1957) was based on a single dose of In, Amata et al. (2015)
310 considered the effects of long term exposure, a situation that is much more relevant to
311 workers exposed to ITO.
312 Sintering of ITO is a solid-state process that aims to generate a technological material
313 by solid-state diffusion and particle annealing. It is an inherently inhomogeneous process that
314 leads to a metastable product (Heward and Swenson, 2007). The observed structure and
315 compositional variability of the ITO powder is consistent with the expected variability in
316 industrial products and the structure of ITO coatings (Thirumoorthi and Thomas Joseph
317 Prakash, 2016). The presence of discrete SnO_2 particles is consistent with incomplete reaction
318 or local supersaturation, as explained by Kim et al. (2006). The particles are coarser than
319 those that are likely to be liberated from ITO coatings, and as the dissolution rate is likely to
320 be a function of the surface area, this implies that the dissolution is likely to be faster than
321 during our experiments. The structure and compositional variation, however, are sufficiently
322 similar to suggest that our results provide a reasonable analogue of ITO particles that are
323 liberated from the production and recycling of flat screen devices.
324 Sintered ITO remains a hardly soluble compound when compared to other In
325 compounds such as In-phosphide, In-arsenide In-trichloride and In-acetate (Chapin et al.,

1995; Oda, 1997; Tanaka, 2004, Lee et al., 2016). Our study demonstrates that ITO is nearly insoluble under simulated upper respiratory tract conditions and in deionized water, while it displays some dissolution in the simulated deep lung and stomach environments. Surprisingly, the In concentrations in the simulated upper respiratory tract conditions (Gamble's solution), deionized water, and deionized water with trypsin display negative correlations with time, suggesting that the metal is removed from solution over time. Robertson (1968) and Smith (1973) documented that In is readily lost from solution unless kept at low pH. They concluded that the metal adsorbs to (or is absorbed into) plastic containers. All of these solutions have near neutral pH, and we consider metal loss to the containers to adequately explain the negative trends.

When inhaled as airborne micro- and nano-particles (Figure 8), our tests with Gamble's solution suggest that ITO is likely to largely remain as solid particles as long as they rest in the upper respiratory tract or tracheobronchial tree. The ITO particles could possibly cause some mechanical irritation but they remain fairly inert in this environment. Very minor differential leaching of Sn is possible, although this is unlikely to be of medical concern. It is interesting that the solubility of In is much lower than in deionised water, indicating that the solubility is negatively affected by the dissolved salts.

Upon contact with the more acidic fluids associated with the deep parts of the lungs (the bronchioles and alveoli), the ITO will release In^{3+} and Sn^{4+} into solution. Our experiments did not plateau at a saturation level, which at least must be higher than the 236 ppm In and 8.5 ppm Sn maxima measured at 480 hours. Our results suggests that In in this environment is able to transfer into the bloodstream for wider dissemination through the human body. The low, but systematic solubility combined with the very long potential residence times for ITO in the deep parts of the lungs suggest that this is the dominant route of transfer of metals into the bloodstream. As outlined above, the United States recommended

inhalation exposure limit indicates that typically 0.67-0.83 mg In could be inhaled an eight hour working day, leading to a total inhalation of 13.4 – 16.6 mg over a period of 20 working days. If 25-45% is considered to accumulate in the deep lungs (Jaques and Kim, 2000), the accumulation over this period would amount to 3.4 – 7.5 mg ITO, of which 2.5 – 5.6 mg would be In. Our experiments reached fluid concentrations of 236 ppm In, which equates to the dissolution of 2.36 mg In in the 10 ml test solution over a period of 20 days. If the amount of extravascular lung water in healthy adults is considered to be 255 ml, as estimated by Wallin and Leksell (1994), the total volume of fluids would be able to dissolve around 60 mg In over this period. While the actual In concentrations that may be reached in the deep lung fluids would depend on the ITO accumulation rates, fluid availability and clearance rates, the scale and scope of our experiments appear entirely realistic for human intake.

The ITO is also likely to slowly decompose in the acid environment of the stomach (Figure 8) leading to the release of In and, to a lesser extent Sn. As for the deep lung environment, the concentrations didn't plateau, and the solubility must at least exceed the measured maximum concentrations of 3 ppm In and 120 ppb Sn. However, it is notable from other laboratory experiments that the solubility of In appears to be strongly pH dependent (Smith, 1973), and it is likely that the dissolution rate will vary substantially during the digestive cycle. Minor further decomposition may occur in the pancreatic juice, where trypsin (and possibly other enzymes) facilitate dissolution. The digestive tract, consequently, offers another route for intake of the In and Sn. However, despite comparable rates of dissolution to the deep lung environment, the much shorter residence times lead to much lower concentrations. The metal transfer through the digestive tract would consequently be much less significant.

While we are not in a position to properly evaluate the wider toxicological effects of ITO, we note that the effects of inhalation is likely not to be restricted to the lung

environment. Over time, In and Sn become mobilized into the bloodstream through the bronchioles and alveoli, and therefore circulate more widely throughout the body. Once taken into the bloodstream, given the low pH of the deep lung fluids and the stomach acid, the In would be likely to take the form of ionic In^{3+} and bind to plasma transferrin (Hosain et al., 1969) before eventually being deposited in the kidneys (Smith et al., 1978). The actual concentrations that can be reached will primarily depend on how fast the deep lung fluids are replenished and cleared. Ionic In in the bloodstream can be expected to have similar health effects as other soluble In-salts, particularly Lewis acids such as In-trichloride. Although In may eventually be excreted (Chen, 2007), it is important to develop an understanding of the potential health effects that could occur more widespread throughout the body through prolonged exposure to ITO.

With the wider environmental dispersion as ITO hits the domestic waste routes, it is likely that adverse health effects may spread much more widely than to ITO factory workers. The most likely people at risk would be scrapyard workers and people involved with recycling of electronic and domestic waste (Zeng et al., 2015), particularly in developing countries where environmental controls are poorly developed (Robinson, 2009; Lim and Schoenung, 2010). While the effects of Sn are well constrained, the largely unknown behavior of In in the surface environment is worrying. It is surprising that In is considered to be fairly harmless, when most of the nearest neighbors in the periodic table (Sn, Cd, Hg, Tl, Pb) are associated with severe adverse health and environmental effects. The wide global dissemination of In leads to concerns about the potential risks that could be caused by the disposal of electronic devices with flat screen displays through the domestic waste routes. Further work is urgently needed to understand how the likely widespread release of In from ITO may affect the environment.

6. Conclusions

While ITO appears to be nearly inert in the upper parts of the respiratory system, In and Sn are likely to be released into fluids in the deep parts of the lungs. At current exposure limits, accumulation rates could potentially reach 50 mg in less than a year for workers exposed to ITO during daily 8 hour working shifts. Concentrations in deep lung fluids could potentially exceed 236 ppm In and 8.5 ppm Sn leading to significant transfer of the metals into the bloodstream. In the digestive tract, In and Sn are also released from ITO in the stomach, where further release may be facilitated by enzymes in the pancreatic juice. However the much shorter residence time indicates a much lower risk of metal uptake through digestion.

Dissolution of ITO from inhaled nano- and microparticles in the deep lung fluids is likely to be the most significant mechanism for transfer of In (and Sn) into the bloodstream. As dissolved metal ions circulate through the human body, the exposure may lead to health damage outside of the environment of the lungs. In this context, the poor knowledge of the environmental properties and potential toxicity of In are immediate causes of concern with respect to the distribution of In-compounds across the human society.

Acknowledgments

This paper was in part supported by the Natural Environment Research Council (NERC, NE/L001896/1). The authors benefited from advice from and discussions with Dr Adam Feldman, sample preparation and X-ray diffraction by Dr Gavyn Rollinson, and ICP-MS analysis by Sharon Uren. Constructive comments from three anonymous reviewers greatly improved the quality of this paper.

References

426 Amata, A., Chonan, T., Omae, K., Nodera, H., Terada, J., Tatsumi, K., 2015. High levels of
427 indium exposure relate to progressive emphysematous changes: a 9-year longitudinal
428 surveillance of indium workers. *Thorax 70, 1040-1046*.
429 Armstrong, J.T., 1995. CITZAF: A Package of Correction Programs for the Quantitative
430 Electron Microbeam X-ray Analysis of Thick Polished Materials, Thin Films, and
431 Particles. *Microbeam Analysis 4, 177-200*.
432 ATSDR, 2016. Minimal Risk Levels (MRLs). *Agency for Toxic Substances and Disease*
433 *Registry*, http,//www.atsdr.cdc.gov/mrls/index.asp.
434 Badding, M.A., Schwegler-Berry, D., Park, J.-H., Fix, N.R., Cummings, K.J., Leonard, S.S.,
435 2015. Sintered Indium-Tin Oxide Particles Induce Pro-Inflammatory Responses In
436 Vitro, in Part through Inflammasome Activation. *PLOS ONE 10, e0124368*.
437 Badding, M.A., Fix, N.R., Orandle, M.S., Barger, M.W., Dunnick, K.M., Cummings, K.J.,
438 Leonard, S.S., 2016. Pulmonary toxicity of indium-tin oxide production facility
439 particles in rats. *Journal of Applied Toxicology 36, 618-626.*
440 Blazka, M.E., 1998. Indium *In: Zelikoff JT, Thomas PT (eds) Immunotoxicility of*
441 *Environmental and Occupational Metals*. Taylor & Francis, London, pp 93-110.
442 Bomhard, E.M., 2016. The toxicology of indium tin oxide. *Environmental Toxicology and*
443 *Pharmacology 45, 282-294*.
444 Böni, H., Widmer, R., 2011. Disposal of Flat Panel Display Monitors in Switzerland, Final
445 Report. *Swiss Federal Laboratories for Materials Science and Technology, Zurich.*
446 Brochu, P., Ducré-Robitaille, J-.F., Brodeur, J., 2006. Physiological Daily Inhalation Rates
447 for Free-Living Individuals Aged 1 Month to 96 Years, Using Data from Doubly
448 Labeled Water Measurements: A Proposal for Air Quality Criteria, Standard
449 Calculations and Health Risk Assessment. *Human and Ecological Risk Assessment,*
450 *An International Journal 12, 675-701*.

Chapin, R.E., Harris, M.W., Hunter, E.S., Davis, B.J., Collins, B.J., Lockhart, A.C., 1995. The Reproductive and Developmental Toxicity of Indium in the Swiss Mouse. *Fundamental and Applied Toxicology 27, 140-148.*

Chen, H., 2007. Exposure and Health Risk of Gallium, Indium, and Arsenic from Semiconductor Manufacturing Industry Workers. *Bulletin of Environmental Contamination and Toxicology 78, 5-9*.

Chonan, T., Taguchi, O., Omae, K., 2007. Interstitial pulmonary disorders in indium-processing workers. *European Respiratory Journal 29, 317-324*.

Colombo, C., Monhemius, A.J., Plant, J.A., 2008. Platinum, palladium and rhodium release from vehicle exhaust catalysts and road dust exposed to simulated lung fluids. *Ecotoxicology and Environmental Safety 71, 722-730.*

Cummings, K.J., Donat, W.E., Ettensohn, D.B., Roggli, V.L., Ingram, P., Kreiss, K., 2010. Pulmonary Alveolar Proteinosis in Workers at an Indium Processing Facility. *American Journal of Respiratory and Critical Care Medicine 181, 458-464.*

Cummings, K., Nakano, M., Omae, K., Takeuchi, K., Chonan, T., Xiao, Y.-I., Harley, R., Roggli, V., Hebisawa, A., Tallaksen, R., Trapnell, B., Day, G., Saito, R., Stanton, M., Suarthana, E., Kreiss, K., 2012. Indium Lung Disease. *Chest 141, 1512-1521*.

Cummings, K.J., Virji, M.A., Park, J.Y., Stanton, M.L., Edwards, N.T., Trapnell, B.C., Carey, B., Stefaniak, A.B., Kreiss, K., 2016. Respirable indium exposures, plasma indium, and respiratory health among indium-tin oxide (ITO) workers. *American Journal of Industrial Medicine 59, 522-531*.

Daugherty, A.L., Mrsny, R.J., 1999. Transcellular uptake mechanisms of the intestinal epithelial barrier. Part one. *Pharmaceutical Science & Technology Today 2, 144-151*.

474 Falk, G., 2012. Sintering of Transparent Conductive Oxides: From Oxide Ceramic Powders
475 to Advanced Optoelectronic Materials *In: Lakshmanan A (ed) Sintering of Ceramics -*
476 *New Emerging Techniques. InTech, pp 587-610.*
477 Fowler, B., Schubauer-Berigan, M., Hines, C., 2009. Indium phosphide and other indium
478 compounds; includes indium phosphide, indium arsenide, indium tin oxide, CIS,
479 CIGS. *International Agency for Research on Cancer Technical Publication 42, 16-24.*
480 Gore, D.J., Patrick, G., 1982. A quantitative study of the penetration of insoluble particles
481 into the tissue of the conducting airways. *The Annals of occupational hygiene 26,*
482 *149-161.*
483 Graedel, T.E., Allwood, J., Birat, J.-P., Buchert, M., Hagelüken, C., Reck, B.K., Sibley, S.F.,
484 Sonnemann, G., 2011. What Do We Know About Metal Recycling Rates? *Journal of*
485 *Industrial Ecology 15, 355-366*.
486 Hamaguchi, T., Omae, K., Takebayashi, T., Kikuchi, Y., Yoshioka, N., Nishiwaki, Y.,
487 Tanaka, A., Hirata, M., Taguchi, O., Chonan, T., 2008. Exposure to hardly soluble
488 indium compounds in ITO production and recycling plants is a new risk for interstitial
489 lung damage. *Occupational and Environmental Medicine 65, 51-55*.
490 Heward, W.J., Swenson, D.J., 2007. Phase equilibria in the pseudo-binary In_2O_3–SnO_2
491 system. *Journal of Materials Science 42, 7135-7140*.
492 Hines, C.J., Roberts, J.L., Andrews, R.N., Jackson, M.V., Deddens, J.A., 2013. Use of and
493 Occupational Exposure to Indium in the United States. *Journal of Occupational and*
494 *Environmental Hygiene 10, 723-733*.
495 Homma, T., Ueno, T., Sekizawa, K., Tanaka, A., Hirata, M., 2003. Interstitial pneumonia
496 developed in a worker dealing with particles containing indium-tin oxide. *Journal of*
497 *Occupational Health 45, 137-139*.

498 Hosain, F., McIntyre, P.A., Poulose, K., Stern, H.S., Wagner, H.N., 1969. Binding of trace
499 amounts of indium-113m to plasma transferrin. Clin. Chim. Acta 24: 69-75.
500 ICDD, 2004. Powder Diffraction file JCPDS PDF-2 Release 2004 (CD-ROM). *International*
501 *Centre for Diffraction Data, Pennsylvania USA. ISSN 1084-3116.*
502 Jaques, P.A., Kim, C.S., 2000. Measurement of total lung deposition of inhaled ultrafine
503 particles in healthy men and women. *Inhalation Toxicology 12, 715-731*.
504 Kim, H., Horwitz, J.S., Kushto, G., Piqué, A., Kafafi, Z.H., Gilmore, C.M., Chrisey, D.B.,
505 2000. Effect of film thickness on the properties of indium tin oxide thin films. *Journal*
506 *of Applied Physics 88, 6021-6025*.
507 Kim, S.-M., Seo, K.-H., Lee, J.-H., Kim, J.-J., Lee, H.Y., Lee, J.-S., 2006. Preparation and
508 sintering of nanocrystalline ITO powders with different SnO_2 content. *Journal of the*
509 *European Ceramic Society 26, 73-80*.
510 Lánský, P., Weiss, M., 2003. Classification of Dissolution Profiles in Terms of Fractional
511 Dissolution Rate and a Novel Measure of Heterogeneity. *Journal of Pharmaceutical*
512 *Sciences 92, 1632-1647*.
513 Lee, K.-H., Chen, H.-L., Leung, C.-M., Chen, H.-P., Hsu, P.-C., 2016. Indium acetate toxicity
514 in male reproductive system in rats. *Environmental Toxicology 31, 68-76*.
515 Lim, S.-R., Schoenung, J.M., 2010. Human health and ecological toxicity potentials due to
516 heavy metal content in waste electronic devices with flat panel displays. *Journal of*
517 *Hazardous Materials 177, 251-259*.
518 Lison, D., Laloy, J., Corazzari, I., Muller, J., Rabolli, V., Panin, N., Huaux, Fo., Fenoglio, I.,
519 Fubini, B., 2009. Sintered Indium-Tin-Oxide (ITO) Particles, A New Pneumotoxic
520 Entity. *Toxicological Sciences 108, 472-481*.

MHLW, 2010. Technical guidelines for preventing health impairment of workers engaged in the indium tin oxide handling process. *Ministry of Health, Labor, and Welfare. Tokyo: Government of Japan, pp. 18.*

Morrow, P.E., Gibb, F.R., Cloutier, R., Casarett, L.J., Scott, J.K., 1957. Fate of indium sesquioxide and of indium-114 trichloride hydrolysate following inhalation in rats *University of Rochester, N.Y. Atomic Energy Project, United States, pp 33.*

Nagano, K., Nishizawa, T., Umeda, Y., Kasai, T., Noguchi, T., Gotoh, K., Ikawa, N., Eitaki, Y., Kawasumi, Y., Yamauchi, T., Arito, H., Fukushima, S., 2011. Inhalation Carcinogenicity and Chronic Toxicity of Indium-tin Oxide in Rats and Mice. *Journal of Occupational Health 53, 175-187*.

Nakano, M., Omae, K., Tanaka, A., Hirata, M., Michikawa, T., Kikuchi, Y., Yoshioka, N., Nishiwaki, Y., Chonan, T., 2009. Causal Relationship between Indium Compound Inhalation and Effects on the Lungs. *Journal of Occupational Health 51, 513-521*.

NIOSH, 1981. Occupational Health Guidelines for Chemical Hazards. *DHHS (NIOSH) Publication 81-123*.

Oda, K., 1997. Toxicity of a low level of indium phosphide (InP) in rats after intratracheal instillation. *Industrial health 35, 61-68*.

Omae, K., Nakano, M., Tanaka, A., Hirata, M., Hamaguchi, T., Chonan, T., 2011. Indium lung—case reports and epidemiology. *International Archives of Occupational and Environmental Health 84, 471-477*.

Omura, M., Tanaka, A., Hirata, M., Inoue, N., Ueno, T., Homma, T., Sekizawa, K., 2002. Testicular Toxicity Evaluation of Indium-Tin Oxide. *Journal of Occupational Health 44, 105-107*.

544 Patrick, G., Stirling, C., 1977. The retention of particles in large airways of the respiratory
545 tract. *Proceedings of the Royal Society of London. Series B, Biological sciences 198,*
546 *455-462.*
547 Radford, E.P., Martell, E.A,. 1977. Polonium-210, Lead-210 ratios as an index of residence
548 time of insoluble particles from cigarette smoke in bronchial epithelium. *In: Walton,*
549 *W.H., McGovern, B. (Eds) Inhaled Particles IV: Proceedings of an International*
550 *Symposium; September 1975; Edinburgh, United Kingdom. Part 2.* Pergamon Press,
551 Ltd, Oxford, United Kingdom, p. 567-581.
552 Robertson, D.E., 1968. The adsorption of trace elements in sea water on various container
553 surfaces. *Analytica Chimica Acta 42: 533-536*.
554 Robinson, B.H., 2009. E-waste, An assessment of global production and environmental
555 impacts. *Science of The Total Environment 408, 183-191*.
556 Ruby, M.V., Davis, A., Schoof, R., Eberle, S., Sellstone, C.M., 1996. Estimation of Lead and
557 Arsenic Bioavailability Using a Physiologically Based Extraction Test.
558 *Environmental Science & Technology 30, 422-430.*
559 Rudnick, R.L., Gao, S., 2003. Composition of the Continental Crust. *In: Holland, H.D.,*
560 *Turekian, K.K., eds. Treatise on Geochemistry*. Pergamon, Oxford, pp 1-64.
561 Shannon, R., 1976. Revised effective ionic radii and systematic studies of interatomic
562 distances in halides and chalcogenides. *Acta Crystallographica Section A 32, 751-*
563 *767*.
564 Smith, A.E., 1973. A study of the variation with pH of the solubility and stability of some
565 metal ions at low concentrations in aqueous solution. Part II. *Analyst 98, 209-212*.
566 Smith, I.C., Carson, B.L., Hoffmeister, F., 1978. *Trace Elements in the Environment: Volume*
567 *5 - Indium*. Ann Arbor Science Publishers.

568 Tanaka, A., 2004. Toxicity of indium arsenide, gallium arsenide, and aluminium gallium
569 arsenide. *Toxicology and Applied Pharmacology 198, 405-411*.
570 Thirumoorthi, M., Thomas Joseph Prakash, J., 2016. Structure, optical and electrical
571 properties of indium tin oxide ultra thin films prepared by jet nebulizer spray
572 pyrolysis technique. *Journal of Asian Ceramic Societies 4, 124-132.*
573 Tuna, O., Selame, Y., Aygun, G., Ozyuzer, L., 2010. High quality ITO thin films grown by
574 dc and RF sputtering without oxygen. *Journal of Physics D: Applied Physics 43,*
575 *055402*.
576 USEPA, 2011. Electronics Waste Management in the United States Through 2009.
577 *U.S. Environmental Protection Agency publication 530-R-11-002*.
578 Wallin, C.J., Leksell, L.G., 1994. Estimation of extravascular lung water in humans with use
579 of 2H2O: effect of blood flow and central blood volume. *Journal of Applied*
580 *Physiology 76, 1868-1875*.
581 Watson, A.Y., Brain, J.D., 1979. Uptake of iron aerosols by mouse airway epithelium.
582 *Laboratory investigation; a journal of technical methods and pathology 40, 450-459*.
583 White, S.J.O., Hemond, H.F., 2012. The Anthrobiogeochemical Cycle of Indium, A Review
584 of the Natural and Anthropogenic Cycling of Indium in the Environment. *Critical*
585 *Reviews in Environmental Science and Technology 42, 155-186*.
586 Zeng, X., Wang, F., Sun, X., Li, J., 2015. Recycling Indium from Scraped Glass of Liquid
587 Crystal Display: Process Optimizing and Mechanism Exploring. *ACS Sustainable*
588 *Chemistry & Engineering 3, 1306-1312*.
589 Zhang, K., Wu, Y., Wang, W., Li, B., Zhang, Y., Zuo, T., 2015. Recycling indium from
590 waste LCDs: A review. *Resources, Conservation and Recycling 104, 276-290*.
591 Zheng, W., Winter, S.M., Kattnig, M.J., Carter, D.E., Sipes, I.G., 1994. Tissue distribution
592 and elimination of indium in male fischer 344 rats following oral and intratracheal

administration of indium phosphide. *Journal of Toxicology and Environmental Health 43, 483-494*.

595 **Figure captions**

596 **Figure 1.** Backscattered electron image (COMP, compositional contrast) of a polished block
597 of the ITO powder. The image shows ITO particles (bright) embedded in epoxy resin (dark)
598 and polished to a flat surface. Particle outlines represent transects through individual
599 particles. Particles are generally rounded aggregates of hollow spheres with high surface to
600 volume ratios. The scale bar is 10 μm.

601

602 **Figure 2**. Concentrations of In (A) and Sn (B) and the In-Sn ratio (C) measured in deionized
603 water in contact with ITO powder. The negative correlations of In and Sn with time are likely
604 to be caused by sorption of metals to the container walls (Robertson, 1968; Smith, 1973).

605

606 **Figure 3**. Concentrations of In (A) and Sn (B) and the In-Sn ratio (C) measured in simulated
607 upper respiratory tract fluids (Gamble's solution) in contact with ITO powder. As for figure
608 2, the negative correlation of In with time is likely to be caused by sorption to the container
609 walls. The substantial decrease in In/Sn over time is a combined effect of In removal and Sn
610 dissolution.

611

612 **Figure 4**. Concentrations of In (A) and Sn (B) and the In-Sn ratio (C) measured in simulated
613 deep lung fluids (the ALF solution) in contact with ITO powder. In and Sn display strong
614 positive correlations with time. The evolution in In/Sn demonstrates selective dissolution of
615 In.

616

617 **Figure 5**. Concentrations of In (A) and Sn (B) and the In-Sn ratio (C) measured in the
618 simulated stomach acid (the PBET solution) in contact with ITO powder. In and Sn display

619 strong positive correlations with time. This environment is not particularly selective in the
620 dissolution of In and Sn.
621
622 **Figure 6**. Concentrations of In (A) and Sn (B) and the In-Sn ratio (C) measured for deionized
623 water with trypsin in contact with ITO. The results indicate that trypsin may facilitate the
624 dissolution of In in the pancreatic fluid to concentrations that are nearly as high as those in
625 the simulated stomach acid.
626
627 **Figure 7**. Comparison of the dissolution of In (A), Sn (B) and the In-Sn ratio (C) for the
628 different experiments illustrated in figures 2-6. The figure highlights the significance of the
629 deep lung environment in the dissolution of inhaled ITO. Concentrations obtained by
630 dissolution in stomach acid and the pancreatic juice (trypsin assisted), while potentially also
631 significant, are limited by the shorter particle residence time.
632
633 **Figure 8**. Schematic illustration of the main routes of ITO uptake in the human body. The
634 most significant route of uptake is through inhalation where the most significant metal
635 transfer is likely to occur in the deep lung fluids. Digestion is another potential route for
636 metal uptake, although the shorter residence time is likely to limit the magnitude of metal
637 transfer.
638

Table 1

Click here to download Table: Andersen et al, Tables.docx

Chemical compound	Chemical formula	ALF solution	Gamble's solution	PBET solution
Magnesium chloride	$MgCl_2$	0.05 g/L	0.10 g/L	-
Sodium chloride	NaCl	3.20 g/L	6.00 g/L	-
Potassium chloride	KCl	-	0.30 g/L	-
Disodium hydrogen phosphate	Na_2HPO_4	0.07 g/L	0.13 g/L	-
Sodium sulphate	Na_2SO_4	0.04 g/L	0.07 g/L	-
Calcium chloride dihydrate	$CaCl_2$ x $2H_2O$	0.13 g/L	0.37 g/L	-
Sodium acetate	$NaC_2H_3O_2$	-	0.57 g/L	-
Sodium hydrogen carbonate	$NaHCO_3$	-	2.60 g/L	-
Sodium citrate dihydrate	$Na_3C_6H_5O_7$ x $2H_2O$	0.08 g/L	0.10 g/L	0.50 g/L
Sodium hydroxide	NaOH	6.00 g/L	-	-
Citric acid	$C_6H_8O_7$	20.80 g/L	-	-
Glycine	NH_2-CH_2-COOH	0.06 g/L	-	-
Sodium tartrate dihydrate	$Na_2C_4H_4O_6$ x $2H_2O$	0.10 g/L	-	-
Sodium lactate	$NaC_3H_5O_3$	0.10 g/L	-	-
Sodium pyruvate	$NaC_3H_3O_3$	0.10 g/L	-	-
Pepsin		-	-	1.25 g/L
Malic acid	$C_4H_6O_5$	-	-	0.50 g/L
Lactic acid	$C_3H_6O_3$	-	-	420 µL/L
Acetic acid	CH_3COOH	-	-	500 µL/L
pH (adjusted with concentrated HCl)		4.5	7.5	4.0

Table 1. Weight and volumes of material for the simulation of the deep lung environment (artificial lysosomal fluid, ALF), the upper respiratory tract (Gamble's solution) and the stomach environment (physiologically based extraction test, PBET). The ALF and Gamble's solutions follow the formulations of Colombo et al. (2008) while the PBET follows Ruby et al. (1996).

Figures 1-8
Click here to download Figure: Andersen et al, Science of total environment figures.pptx

Andersen et al. Figure 1 ½ page width

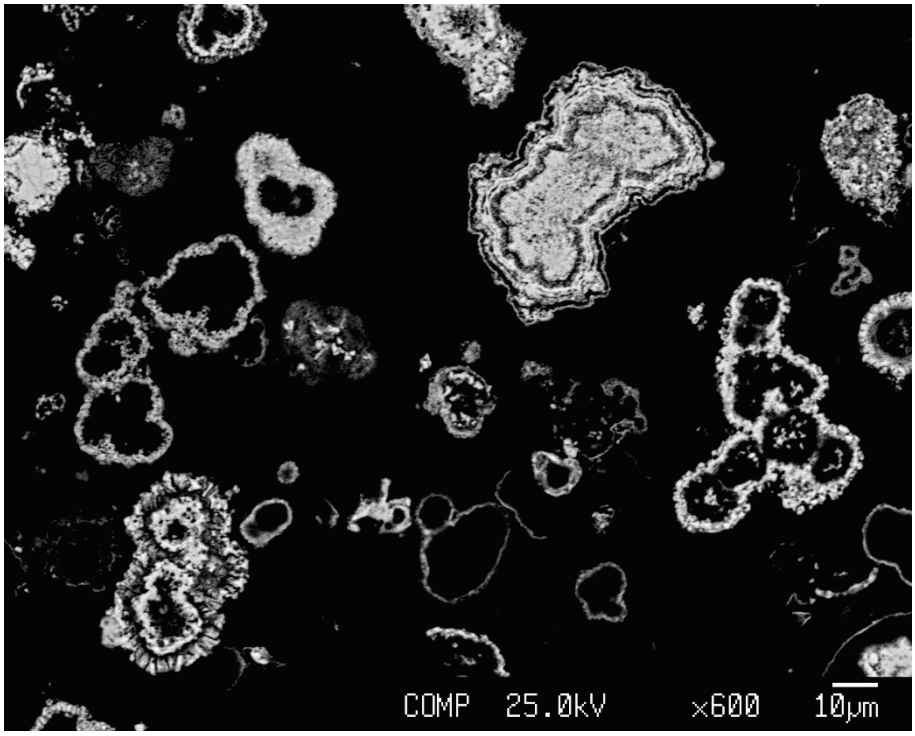

Andersen et al. Figure 2 ½ page width

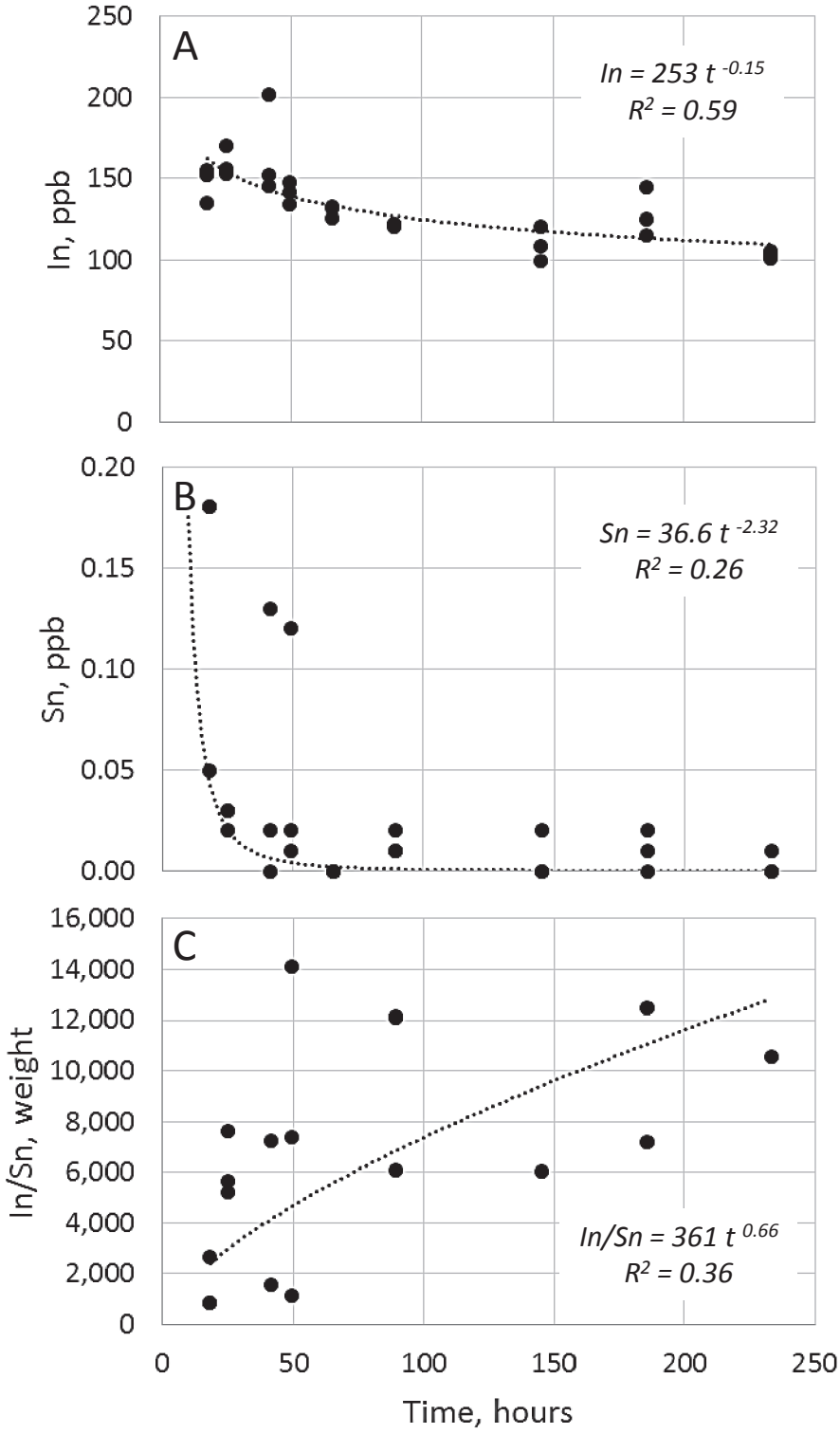

Andersen et al. Figure 3 ½ page width

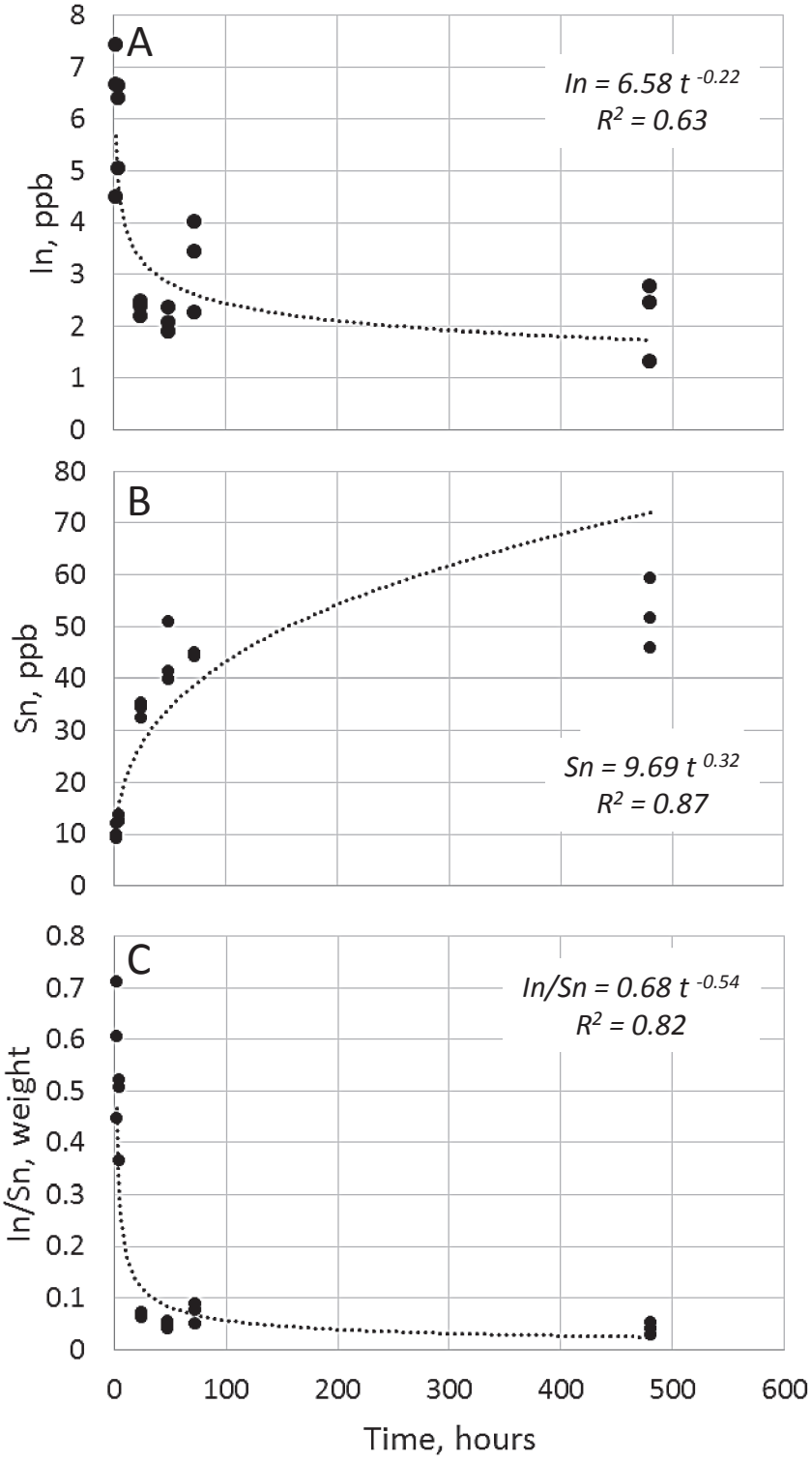

Andersen et al. Figure 4 ½ page width

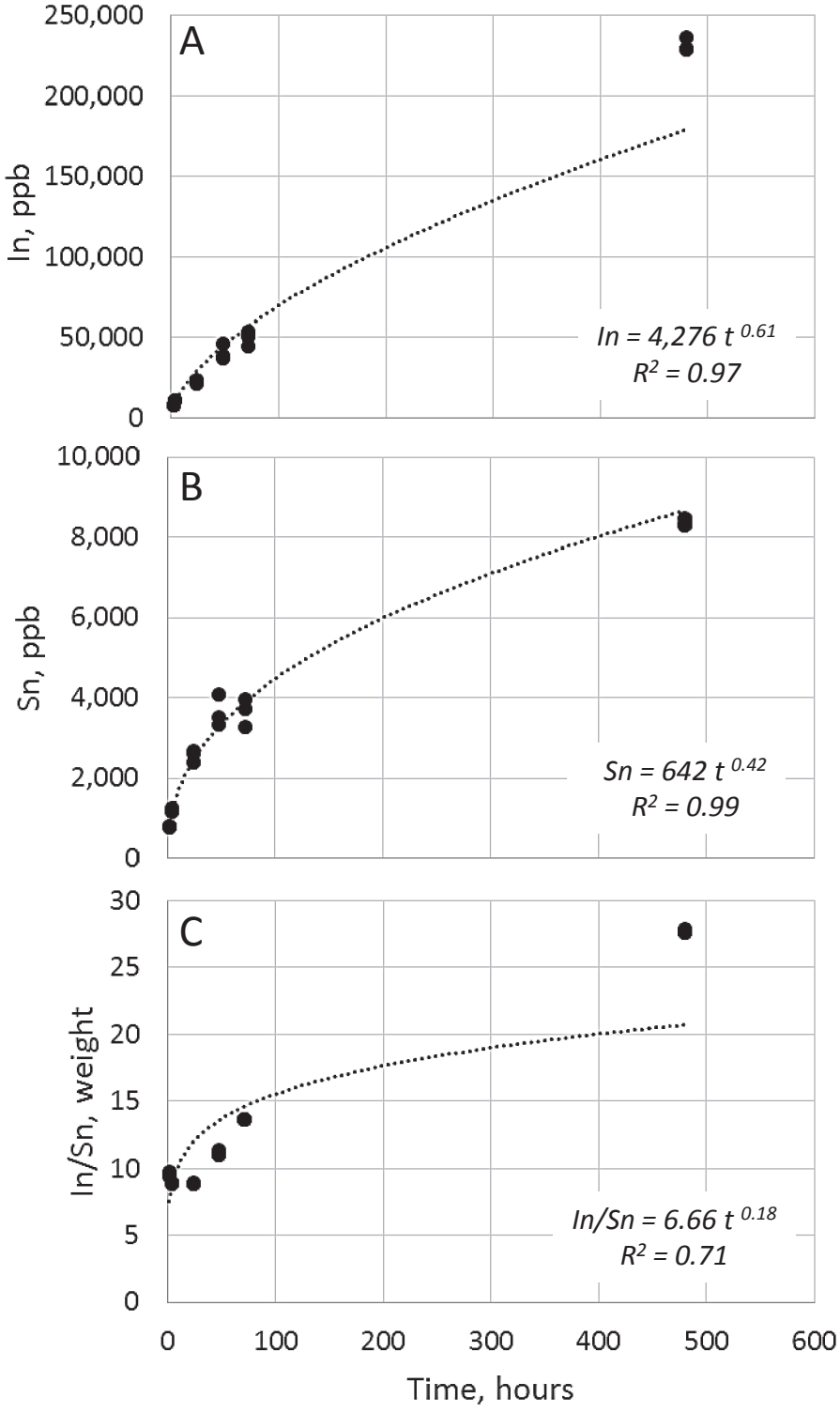

Andersen et al. Figure 5 ½ page width

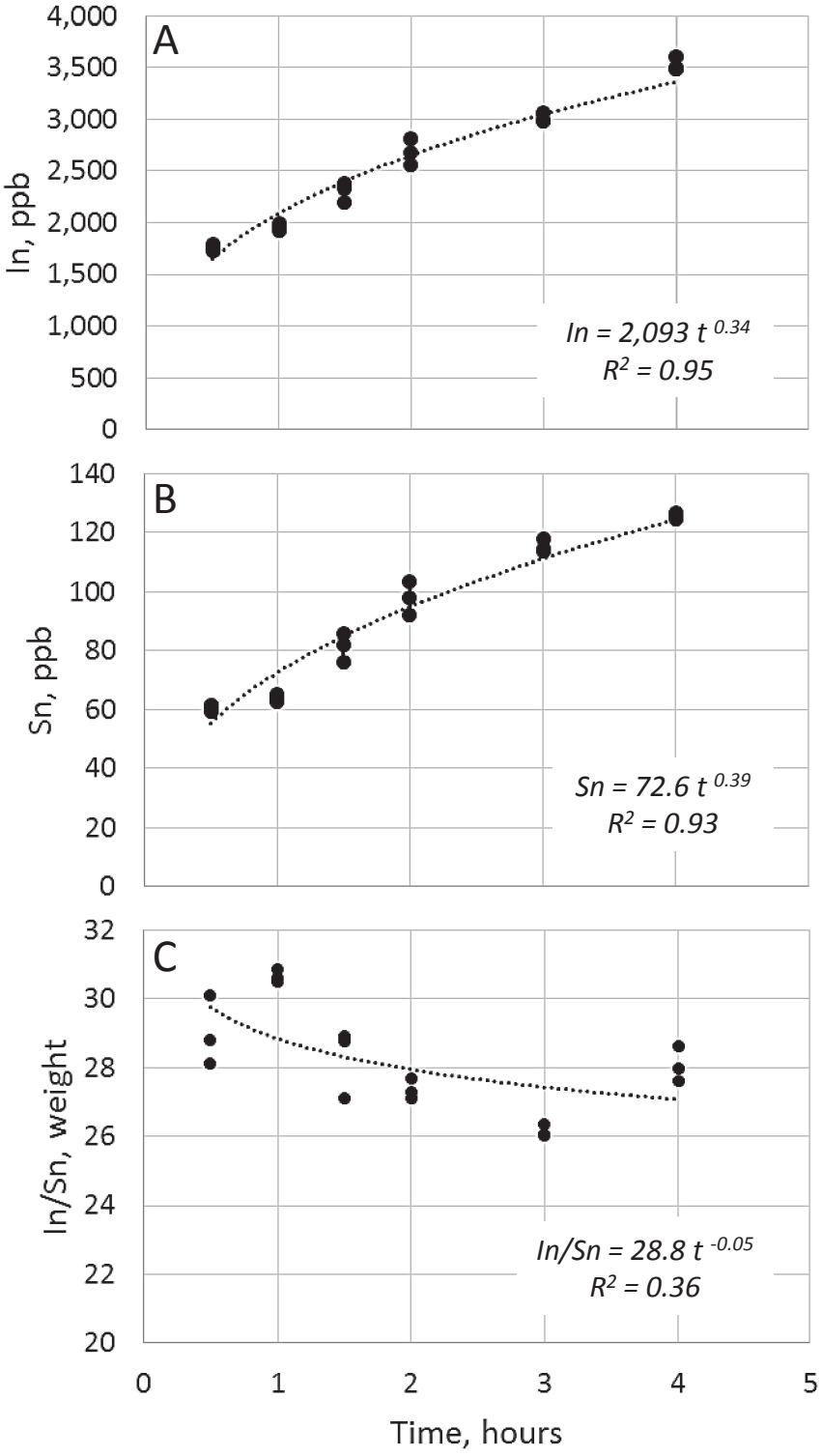

Andersen et al. Figure 6 ½ page width

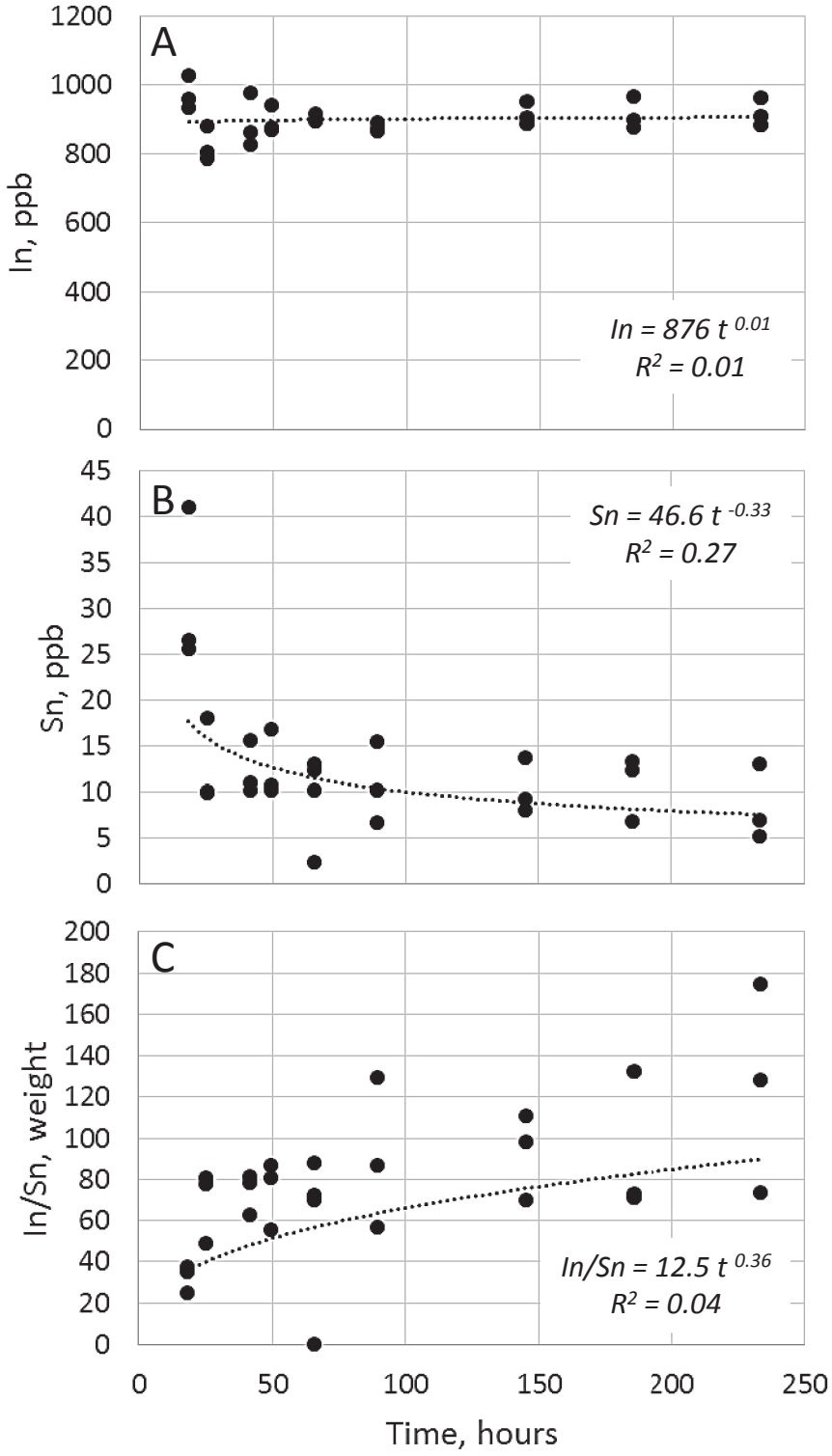

Andersen et al. Figure 7 ½ page width

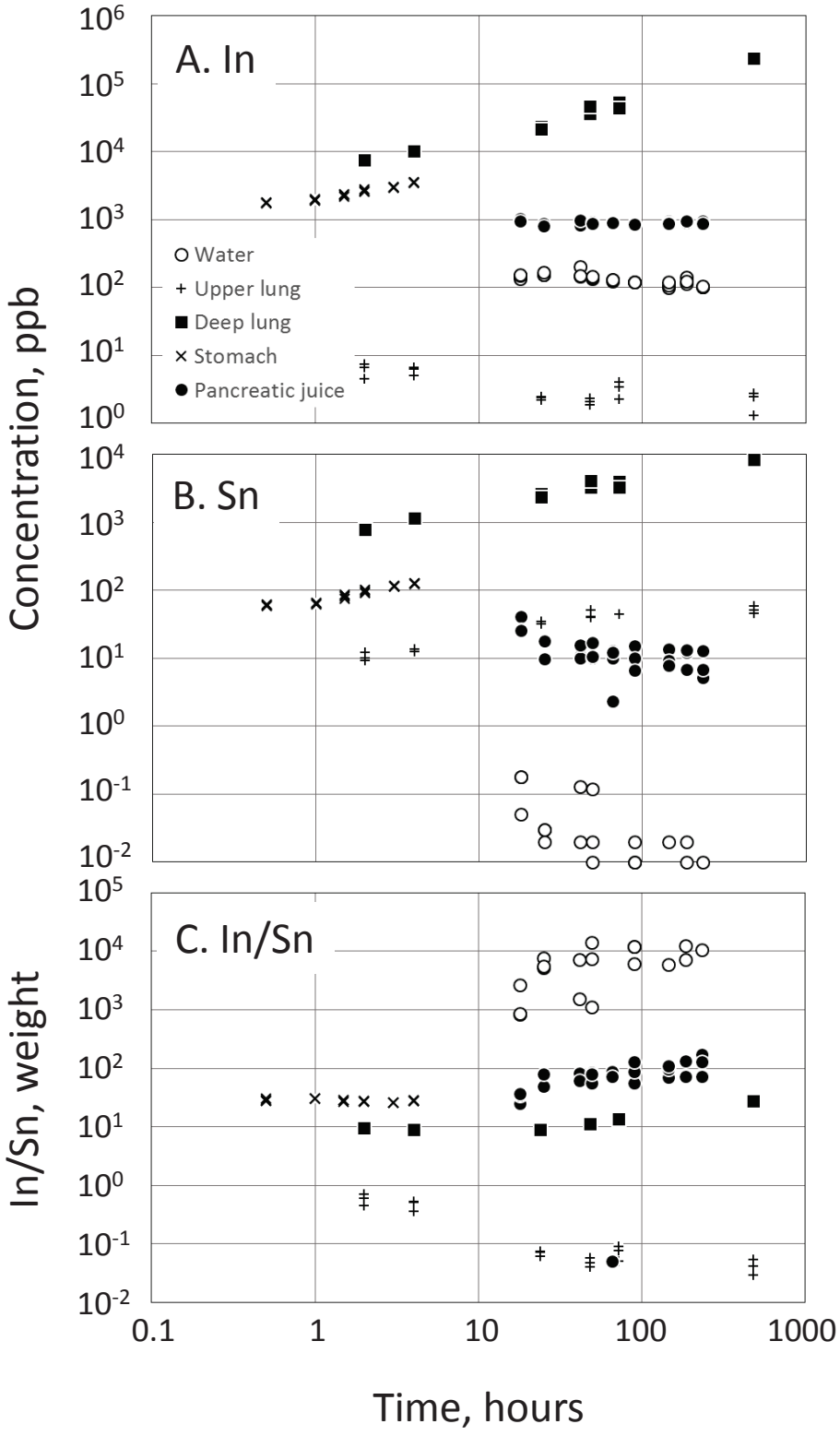

Andersen et al. Figure 8 Full page width